MNE 24 (2024) 100269

Contents lists available at ScienceDirect

Micro and Nano Engineering

journal homepage: www.sciencedirect.com/journal/micro-and-nano-engineering

Superhydrophobic and oleophobic Nylon, PES and PVDF membranes using plasma nanotexturing: Empowering membrane distillation and contributing to PFAS free hydrophobic membranes

Eleftherios Manouras [a], Dimosthenis Ioannou [a,b], Angelos Zeniou [a], Andreas Sapalidis [a], Evangelos Gogolides [a,*]

[a] Institute of Nanoscience and Nanotechnology, NCSR "Demokritos", Aghia Paraskevi, 15341 Attica, Greece
[b] School of Mechanical Engineering, National Technical University of Athens, Zografou, 15780 Attica, Greece

ARTICLE INFO

Keywords:
Superhydrophobic surfaces
Plasma technology
Etching
Deposition
Membrane Distillation

ABSTRACT

As freshwater demand is constantly increasing, water purification via membrane distillation (MD) emerges as a promising water production technology, especially when combined with the use of superhydrophobic membranes. Here, following our previous work [1] we extend our universal, environmentally friendly, plasma nanotexturing and hydrophobization technology for rendering practically any type of membrane superhydrophobic and oleophobic. Thus, we render three commercial porous membranes superhydrophobic, namely, polyvinylidene (PVDF 0.45 μm) (initially hydrophobic), polyethersulfone (PES 1.20 μm) and nylon (NY 1.20 μm) (both initially hydrophilic). We demonstrate superhydrophobic, superoleophobic (down to 40mn/m surface tension) and oleophobic properties (down to 30mN/m surface tension) for PVDF, PES and Nylon membranes thus paving the way for their use with low surface tension waste streams. Moreover, the technology presented herein not only improves existing hydrophobic membranes but may lead to elimination of the use of Teflon-like fluorinated hydrophobic membranes altogether in the future, thereby contributing to the PFAS (Per and Poly Fluoro Alkyl Substances) and Teflon-like membrane use reduction. We subsequently evaluated the performance of the treated membranes in direct contact membrane distillation (DCMD) for desalination of sea-like water (35 g/L NaCl). All membranes showed enhanced water flux with an increase of >13% compared to the pristine hydrophobic PVDF membranes for at least 2 h of continuous operation, with salt rejection exciding 99.99%.

1. Introduction

Access to clean water is recognized as a basic human right by the United Nations but remains unavailable or scarce to a large portion of world population [2,3], while water resources are being depleted at an alarming rate [4]. In the future, the demand for larger quantities of freshwater will increase exponentially due to population growth, enhanced living standards, and the expansion of industrial and agricultural activities. Mature technologies like membrane based and thermal desalination as well as emerging ones such as water harvesting from atmospheric moisture/fog [5,6] are possible solutions to the problem. Membrane Distillation (MD) is a particularly promising method currently under investigation worldwide as an alternative and often complementary efficient solution for the treatment of challenging feedwaters [7].

Membrane distillation is a thermally driven and non-isothermal separation process that uses a hydrophobic porous membrane from which only vapor molecules can pass from a hot stream (feed) on one side to a cold stream (permeate) on the other [8–10], without the need of applying hydraulic pressure. This leads to the worldwide exploration of the MD technique as an alternative to conventional methods (Reverse Osmosis - RO, Multi effect distillation -MED etc.). MD has the potential for low cost and energy efficiency [7], since it uses low temperatures and can be combined with solar energy heating [9,11]. Compared to other membrane-based methods, MD can theoretically yield a perfect 100% rejection of inorganic ions, macromolecules and other non-volatile compounds [9]. There are four main MD configurations which are direct contact membrane distillation (DCMD), air gap membrane distillation (AGMD), vacuum membrane distillation (VMD) and sweeping gas membrane distillation (SGMD) [12]. In the case of DCMD which

* Corresponding author.
E-mail address: e.gogolides@inn.demokritos.gr (E. Gogolides).

https://doi.org/10.1016/j.mne.2024.100269
Received 13 January 2024; Received in revised form 21 June 2024; Accepted 28 June 2024
Available online 2 July 2024

was used in this work, the two aqueous solutions (feed and permeate) are in contact with the porous membrane, which separates them, on either side. Evaporation takes place on the membrane surface on the feed side while due to the lower temperature on the opposite side condensation occurs leading to an increase in permeate flow. Feed maximum temperatures usually range from 60 to 80 °C, but MD can also operate even at 40 °C if the temperature difference is sufficient.

There are still some membrane related challenges that need to be addressed before MD becomes a viable global industrial method for water treatment. These are mainly: i) Wetting, ii) Scaling and iii) Fouling. To maintain the membrane in a state of non-wetting for long operating periods, the membranes must be hydrophobic and actively prevent liquid passing through their pores, as well as capillary condensation. Typically, Teflon-like (and therefore PFAS containing) membranes are used such as PTFE and PVDF. Recently, superhydrophobic membranes have attracted attention yielding better results in MD processes [9,13–15].

Scaling is a very big challenge in MD and other desalination methods when treating high salinity (>50,000 TDS or > 50 g/L) industrial wastewater where in reverse osmosis (RO) is not feasible because the hydraulic pressure cannot exceed the membrane burst pressure [16]. During MD, dissolved compounds accumulate as the water evaporates, and eventually lead to the formation of a precipitated salt layer on the membrane surface, a phenomenon also known as mineral scaling [16]. The scaling deposition reduces process efficiency or leads to process failure through wetting [13,17].

Finally, fouling is an umbrella term that can include organic fouling, inorganic fouling and biological fouling. Failure due to fouling is common in membrane distillation and its applications, where particles in the feed solution accumulate on the membrane surface and block the membrane pores (e.g., proteins), reducing the permeability flux and posing the risk of pore wetting [13,18].

Plasma polymerization has been used to deposit hydrophobic fluorinated coatings both on flat membranes, and in hollow fiber membranes with very promising applications in MD [19,20]. In addition, such coatings successfully hydrophobized initially hydrophilic membranes. Such membranes were used in MD giving high desalination fluxes, and in a cross flow hollow fiber MD configuration showed high resistance to scaling in long term operation [21–23]. Yet, no superhydrophobicity/superoleophobicity was obtained. Recently superhydrophobic membranes have been proposed by our group as a potential improvement in wetting, fouling and scaling [1,24].

Herein, we extend our work presented by Ioannou et al. [1] on the plasma nanotexturing and plasma hydrophobization technology for membrane treatment by rendering for the first time superhydrophobic, superoleophobic (down to 40mn/m surface tension) and oleophobic (down to 30mn/m surface tension) three commercial membranes, one initially hydrophobic (PVDF) and two initially hydrophilic (PES, Nylon). In the literature, the PES membrane has been rendered superhydrophobic before only by our collaborators from Max Planck in a previous publication [25] by a different wet technology involving nanofilament growth. We therefore show that plasma nanotexturing and plasma hydrophobization, which are both dry technologies, can improve dramatically the properties of existing hydrophobic membranes such as PVDF, and can convert to superhydrophobic and oleophobic widely used commercial membranes such as PES and Nylon, thus paving the way for their use with low surface tension waste streams. Moreover, rendering of PES and Nylon membranes as superhydrophobic and oleophobic, combined with the rendering of CA (Cellulose Acetate) membranes superhydrophobic in our previous work [1] allows us to claim that with our technology one can in the future avoid the use of fluorinated membranes altogether thus contributing to the Teflon-like and PFAS membrane use reduction. We then evaluate these membranes via DCMD and present robust performance and enhanced water desalination processes even using membranes that were initially unusable for MD. After the MD experiments the originally hydrophobic membrane showcased a 13% increased DCMD flux while their hydrophilic counterparts were also successfully used for the same experiments with a high salt rejection of 99.99% in each case.

2. Experimental

2.1. Membrane materials

In the present work three different types of 142 mm diameter flat sheet membranes with average thickness of 150–200 μm were purchased from Dorsan Filtration [26] (see also Fig. S1 Supplementary Material). The first type of membrane used was a hydrophobic polyvinylidene fluoride (PVDF) membrane with an average pore size of 0.45 μm and an average thickness of 140–250 μm. The structure of these membranes consists of a thick support layer of fibers between two thin layers of porous PVDF polymer and possesses a unique combination of properties such as chemical resistance, high strength and excellent thermal stability. The second type of membranes was the hydrophilic nylon (NY) membranes made on a spunbond polyester support for mechanical resistance [26] with an average pore size of 1.2 μm and an average thickness of 150 μm. Its structure is similar to that of PVDF in that it has a sandwich-like form with a support layer consisting of nylon microfibers between two thin, porous, sponge-like layers of nylon. Finally, the third type of membrane used was also a hydrophilic membrane made from pure polymer polyethersulfone (PES) [26] (see also Fig. S2 Supplementary Material) with an average pore size of 1.2 μm and an average thickness of 150 μm. The structure of the membrane is different from the other two consisting of a web-like porous mesh throughout its length and thickness and is characterized by its durability and low protein binding according to the manufacturer.

2.2. Plasma treatment of membranes

The plasma reactor that was used in this work was a DRIE (Deep reactive ion etching) inductively coupled plasma (ICP) reactor built at the Institute of Nanoscience and Nanotechnology [27] equipped with a double helical source (at 13.56 MHz). All membranes were treated inside this reactor (see also Fig. S3 Supplementary Material). The plasma process comprises two steps: a) first the plasma nanotexturing step using O_2 plasma during which a thin surface layer (of a few μm in thickness) of the membrane is etched away (removed), while simultaneously the membrane is roughened in the micro and nano scale (micro-nanotexturing) due to simultaneous co-sputtering of a quartz electrode in this particular reactor (see also discussion when the membrane morphology is discussed), b) the hydrophobization step with plasma deposition of a thin fluorocarbon film using C_4F_8 (a fluorocarbon) plasma. The approximate thickness of the fluorocarbon (~50-100 nm, see Table 1) is measured before treatment using a flat silicon wafer and measuring the thickness using ellipsometry. The plasma processing conditions are shown in Table 1.

Table 1
Conditions for O_2 plasma nanotexturing and C_4F_8 deposition in the plasma reactor.

Gas type	O_2	C_4F_8
Plasma process type	Etching	Deposition
Gas Flow	100 sccm	17.2 sccm
Process Pressure	6 mTorr	26 mTorr
Source power	300 W	500 W
Bias electrode power	300 W	0 W
Bias electrode voltage	200 V	0
Electrode temperature	15 °C	15 °C
Operating frequency	13.56 MHz	13.56 MHz
Optimal operation time	PVDF – 3 min PES – 2 min NY – 1 min	PVDF – 1:30 min (~50 nm) PES and NY – 3 min (~100 nm)

2.3. Membrane characterization

2.3.1. Morphological characterization

For the characterization of the morphology/topography of the surfaces treated with plasma, a JEOL JSM-7401F FEG scanning electron microscope (SEM) was used with beam voltage of 2.5 kV and a beam current of 2–10 μA after coating with a conductive platinum coating of typical thickness of 5–6 nm on a flat substrate.

2.3.2. Static contact angle SCA, contact angle hysteresis CAH, and surface tension

The Kruss DSA 100 Contact Angle Measurement System was used to measure the contact angles of surfaces with static 5.0 μL water droplets. For this measurement of contact angle hysteresis, a drop of a specific volume (2.0 μL) is initially deposited, which is increased by subsequent infusion of liquid (2.0 μL/s), thus measuring the advancing angle, while subsequent liquid suction allows the receding contact angle measurement to be extracted. Subtracting these two angles leads to the hysteresis angle. Furthermore, isopropanol-in-water mixtures with surface tensions from 72 mN/m (surface tension of water) to as low as 30 mN/m at RT (~25 °C) were prepared in order to simulate oils or low surface tension aqueous solutions in general. Using the same device, the WSCA was measured to evaluate the wetting properties of the membranes with lower surface tension liquids.

2.3.3. Liquid Entry Pressure

The Liquid Entry Pressure (LEP) of a porous hydrophobic membrane is the minimum pressure that must be applied to a dry membrane to allow liquid to penetrate through the largest pore of the membrane [28]. LEP is a preliminary indication of the level of wetting that a membrane exhibits against various liquid solutions. In its simplest theoretical form based on the Young-Laplace equation the LEP is defined as follows:

$$\mathrm{LEP} = -\frac{\beta \bullet \gamma \bullet \cos\theta}{r_{max}} \tag{1}$$

where β is a coefficient of pore geometry (with $\beta = 1$ for cylindrical pores and $0 < \beta < 1$ for non-cylindrical pores), γ is the surface tension of the liquid, θ is the contact angle measured on the liquid side, and r_{max} is the maximum pore size of the membrane [29].

2.3.4. Porosity

Porosity is defined as the ratio of the volume of the space occupied by air within the material to the total volume of the material. One way to measure the porosity of a membrane is by relative weight measurement before and after immersion in isopropanol, then the porosity ε can be calculated according to the formula:

$$\varepsilon = \frac{\frac{w_{iso+pol} - w_{pol}}{\rho_{iso}}}{\frac{w_{iso+pol} - w_{pol}}{\rho_{iso}} + \frac{w_{pol}}{\rho_{pol}}} \tag{2}$$

Where, w_{pol} is the weight of the membrane, $w_{iso+pol}$ is the weight of the membrane immersed in isopropanol, ρ_{iso} is the density of the isopropanol and ρ_{pol} is the density of the polymer of the membrane material [28].

2.3.5. Tortuosity

The deviation of the pore structure from the ideal linear, cylindrical shape is called tortuosity. Porosity value of 1, corresponds to a membrane with perfectly cylindrical pores [30]. Tortuosity can be calculated empirically from the following equations [31,32] which are the most accurate for calculating tortuosity [1,33,34] depending on the porosity of the membrane [34]:

$$\tau = \frac{(2-\varepsilon)^2}{\varepsilon} \; for \; \varepsilon < 70 \tag{3}$$

$$\tau = \frac{1}{\varepsilon} \; for \; \varepsilon \geq 70 \tag{4}$$

2.4. Direct contact membrane distillation (DCMD) setup

A lab-scale setup for direct contact membrane distillation (DCMD) was used to evaluate the performance of plasma-treated membranes. The DCMD setup has been described in [18,35]. The flow of pure water condensed in the permeate side of the membrane is measured with a high-precision electronic mass flow meter, while the salinity of both flows is determined with two conductivity meters [28]. The operating conditions are listed in Table 2. The distillation flux during the DCMD process is calculated experimentally from the following equation [36]:

$$\mathrm{Flux} = \frac{\text{Permeate flowrate}}{\text{Membrane Area}} \tag{5}$$

And it is measured in liters per square meter per hour (or LMH).

Using the conductivity of the permeate and feed water the salt rejection can be easily calculated from the Eq. [1]:

$$\text{Salt Rejection} = \left(1 - \frac{\text{Permeate conductivity}}{\text{Feed water conductivity}}\right) \bullet 100\% \tag{6}$$

Both the commercial and plasma-treated membranes were tested using this DCMD setup. This setup provided a continuous test for at least 2 h.

3. Experimental process and results

3.1. Membrane wetting properties before and after plasma treatment

The three membranes used were first measured for their contact angles in their pristine state and then again after the plasma treatment, as shown in Table 3 below. Notice that the PVDF membranes are initially hydrophobic but not superhydrophobic since the CA is below 150° and the hysteresis angle is above 10°. On the other hand, the PES and NY membranes were superhydrophilic, meaning their CA was below 10°. Different times for the nanotexturing step in O_2 plasma and the hydrophobization step via plasma deposition in C_4F_8 plasma were tested while evaluating the membranes after treatment regarding their superhydrophobicity. The criteria for successful processing were: a) contact angle >150° and hysteresis angle <10°, b) LEP value ≥1 bar; we posed this strict requirement to make sure the membranes would not wet when subjected to equivalent pressure drop of flowing saline water stream, c) that the top layer of the membrane is not completely etched in the oxygen plasma during the nanotexturing step, i.e. it is not exposing the support of the membrane (in the cases of PVDF and NY membranes which have such a top layer as mentioned in 2.1, see also Fig. S4a and S4b Supplementary Material). The results of these tests can be seen in Table S5 in Supplementary Material.

The plasma treatment of the membranes causes a widening of the surface pores and a thinning of the membrane resulting in a decrease of the LEP value. Therefore, even though the measured LEP of the untreated PVDF was 1.20 ± 0.05 bar, the treated membrane exhibited a

Table 2
Operating parameters for the DCMD experiment.

Variables	Values
Feed inlet temperature	80 °C
Feed flow rate	~105 mL/min
Permeate inlet temperature	15 °C
Permeate side flow rate	~95 mL /min
Effective membrane area	21.02 cm^2
NaCl concentration	35 g/L
Feed conductivity @ 22 °C	~50 mS/cm
Transmembrane pressure	<50 mbar
Test duration	2 h

Table 3
Wetting properties of membranes before and after treatment.

Membrane (mean pore size)	Wetting Properties before treatment SCA/CAH	Wetting Properties after treatment SCA/CAH
PVDF (0.45 μm)	142° ± 4° / >15°	168° ± 0.9° / < 5°
PES (1.20 μm)	0°	164° ± 1.3° / < 5°
NY (1.20 μm)	0°	164° ± 1.1° / < 5°

lower LEP of around 1.09 ± 0.02 bar. The PES membranes having already bigger pores than the PVDF membrane were treated for a lower etching time. A nanotexturing time of two minutes for the PES and one minute for the NY were deemed optimal since their LEP values were above 1 bar and after the deposition treatment both were rendered superhydrophobic.

Wetting of the membranes was tested for various surface tension liquids. Solutions of DI water and isopropanol were prepared with various percentages including 0%, 4%, 6%, 14% and 27% *v*/v of isopropanol corresponding to surface tensions of 72, 60, 50, 40 and 30 mN/m respectively (see also Fig. S6 Supplementary Material). The results of those measurements are seen in Fig. 1. The membranes may resist wetting for solutions with surface tension at least 40mN/m, thus showing superhydrophobic, superoleophobic properties down to 40mN/m, and oleophobic properties down to 30mN/m.

The above results show the potential of plasma treated membranes to be used in desalination or wastewater treatment/purification where there are surfactants, oils, acids, or bases, or biofoulants that would reduce the surface tension and in addition shows the superiority of our membranes compared to the pristine hydrophobic membrane.

3.2. Morphological characterization of membranes

The surface morphology of the membranes after etching at the optimal processing conditions was observed for various magnifications and angles with a scanning electron microscope (SEM) and is shown in Figs. 2, 3, 4 below for each membrane type. We note that the hydrophobization step by deposition does not change the topography as only a few tens of nm of fluorocarbon polymer is deposited (~50 for the PVDF membrane and ~ 100 nm for the PES and NY membranes).

The mechanism of topography alteration during the nanotexturing step has been discussed in our previous works [13,37,38], but here a quartz cover plate of the electrode is used rather than a metallic or

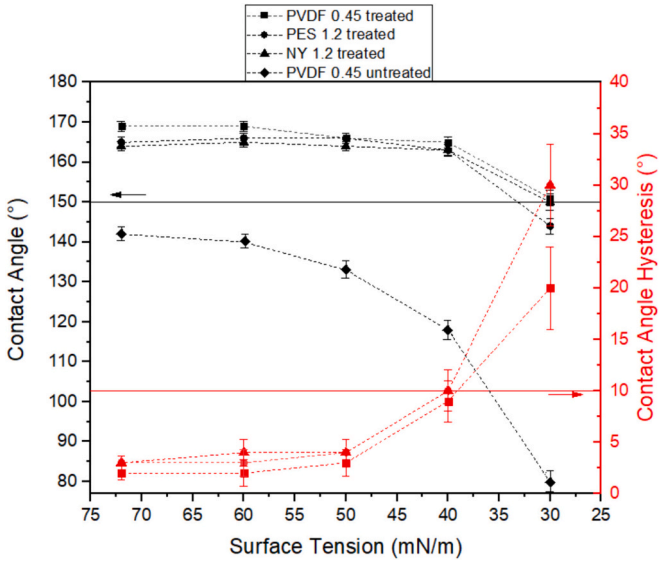

Fig. 1. Results of the CA and hysteresis measurements with different surface tension liquids for the plasma treated membranes.

alumina electrode cover plate. Briefly, ions, accelerated by the plasma-surface potential-difference impinge on both the target and the membrane perpendicular to their surface. They sputter the quartz cover plate (hence the cover plate can be thought of as a target) and etch the membrane. During etching, the sputtered quartz inhibitors arrive on the membrane surface simultaneously with etching radicals and ions (e.g., O radicals, O2+ ions), and block locally the membrane etching. Thus, a local inhibitor nanomask results in a columnar nanostructure formation as the area around the nanomask is etched faster by the oxygen plasma, a process which we have termed "nanoinhibit" process [39] and resembles the "nanograss" formation observed during etching in microelectronics. After the etching step with O_2, by switching the gas to octafluorocyclobutane (C_4F_8) we alter the surface chemistry by deposition of a thin hydrophobic layer (~50–100 nm) [40] which grants superhydrophobicity to our membranes. A schematic of the mechanism of nanotexture formation is shown in Fig. 5 [39,41]. The same process has been used for roughness creation in various polymeric materials in other plasma reactors, and it is extremely reproducible [1,37,42].

3.3. Direct contact membrane distillation performance

The membranes that were evaluated and deemed optimal using the two-step treatment involving the deposition with C_4F_8, described in paragraph 3.1, were used in a DCMD setup for desalination (see also Fig. S7a and S7b Supplementary Material) of sea-like water against a 35 g/L NaCl aqueous solution. The temperature of the feedwater was fixed at 80° C while the permeate flow was fixed at 15° C.

The plasma treated PVDF membrane exhibit a higher flux (19.4 LMH) in comparison to their untreated counterpart (17.2 LMH) by an average enhancement of 13%. The two initially superhydrophilic PES and NY membranes which were unusable in DCMD processes, presented a stable performance after the plasma treatment with no wetting issues observed during desalination and exhibited a 17.9 LMH and 10.5 LMH flux, respectively (Fig. 6).

All membranes demonstrated an excellent salt rejection rate > 99.99% with no signs of a decline in terms of performance throughout the whole DCMD process. Additionally, they maintained their superhydrophobic properties when re-evaluated after the desalination tests demonstrating the durability of the proposed method.

3.4. Other membrane properties

The effect that the plasma treatment has on the porosity and the tortuosity of the membranes was tested and the results are reported in Table 4 using Eqs. (2)–(4). The values of the untreated and treated membranes are not very different, highlighting that plasma processing is a surface process, and the thinning of the membrane is reflected in the slightly increased porosity and slightly reduced tortuosity. Thus, apart from the surface topography and surface energy change the other main effect is the thinning of the membrane due to plasma etching.

3.5. Results and discussion

After a series of tests under different plasma treatment conditions, all three membranes were successfully rendered superhydrophobic / superoleophobic / oleophobic, regardless of their initial wetting state. This was confirmed using solutions with lower surface tension than water and they maintained superhydrophobic/ superoleophobic for solutions with surface tension as low as 40 mN/m, and oleophobic for solutions down to 30mN/m. Morphological observations through SEM images revealed roughness induced by the O_2 etching step, and notably, no complete etching/removal of the top layer was detected for the PVDF and NY membranes, but only thinning of the membrane. Additionally, LEP evaluation tests indicated that all membranes remained above the critical 1 bar threshold, confirming that the plasma etching did not remove the top layer and did not expose the support material of the

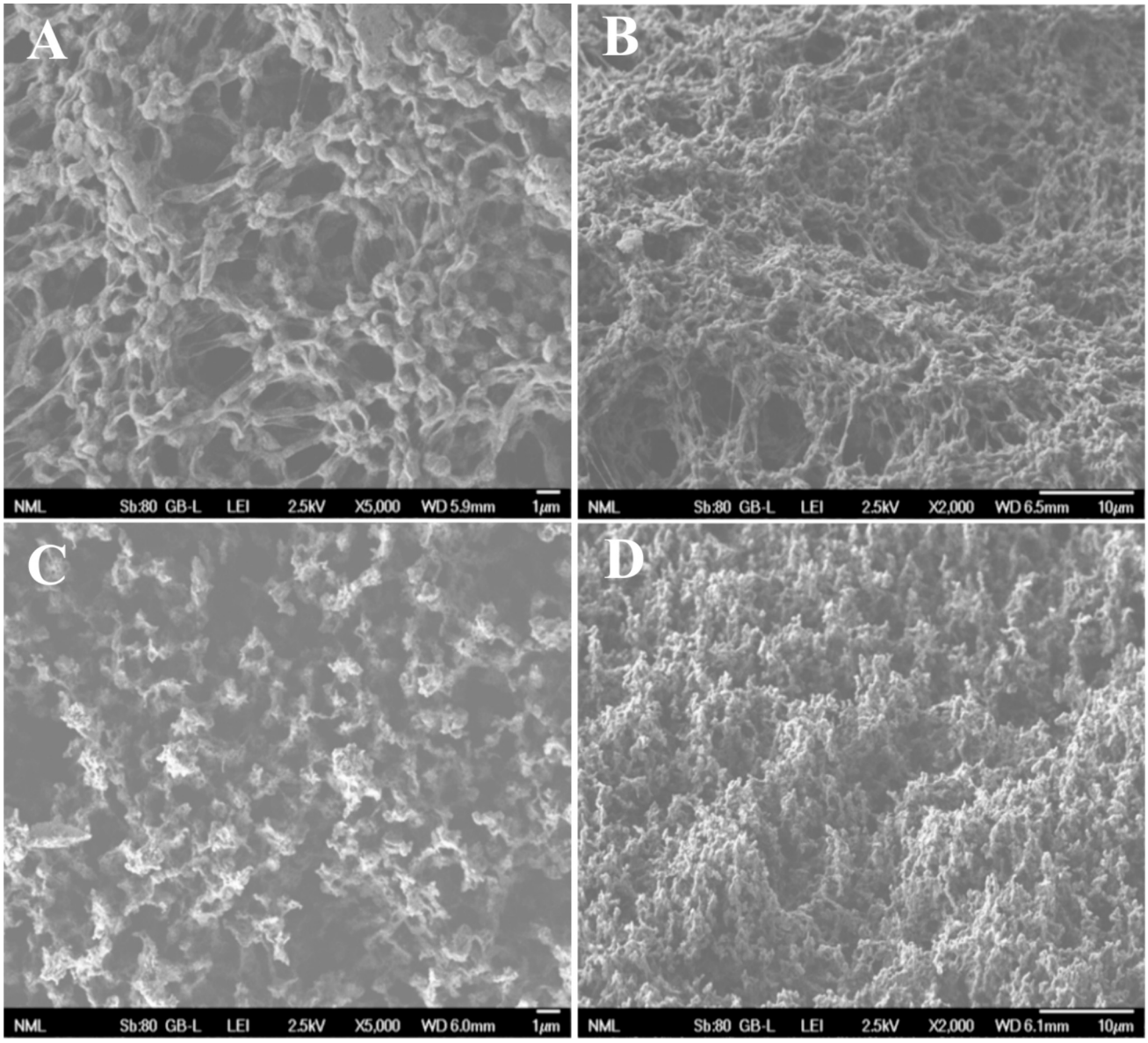

Fig. 2. SEM images of the PVDF membrane morphology A) Untreated top down (x5000 magnification), B) Untreated at 45° angle (x2000 magnification), C) After treatment for 3:00 min with O_2 top down (x5000 magnification) and D) After treatment for 3:00 min with O_2 at 45° angle (x2000 magnification).

PVDF and NY membranes.

The MD experimental results demonstrated a 13% improvement in permeate flux for the PVDF membrane over a 2-h operation, with a salt rejection rate > 99.99%. This improvement is consistent with previous studies [1] under similar plasma treatment conditions, which reported flux increases of 10–15%. As shown in our previous work [1,24], membranes exhibit more stable performance during MD following our treatment. Therefore, we anticipate that the PVDF membrane would show even greater performance improvements over longer durations, as the present study we did not encounter significant scaling or fouling due to the short operation time.

In an attempt to theoretically explain the increase in flux after our treatment we connect variations in thickness, porosity and tortuosity (see Table 4) using Eq. (7) in the transition region, where r is the pore radius, D the diffusion coefficient and δ the membrane thickness, [33,34].

$$Flux \sim \frac{\varepsilon}{\delta \bullet \tau} \bullet f(T, P, D, r) \tag{7}$$

where, function f varies little with plasma processing being related to membrane average properties). The detailed form of the equation and results are shown in Supplementary Material (section S8). Eq. (7) shows that while plasma treatment primarily modifies the surface, even minimal thinning of the membrane can contribute to increased flux [32,34]. As seen in the S8 section in Supplementary Material, we did a comparison between the PVDF untreated and treated theoretical flux and saw that the expected flux increase with our conditions would be approximately 15–20% [33,43–46]. Not being able to accurately measure thickness from cross sectional SEM we consider the theoretical prediction very close to the experimental 13% improved flux value.

For the initially superhydrophilic PES and NY membranes, the plasma treatment successfully rendered them superhydrophobic, enabling their use in MD with fluxes of 17.9 LMH and 10.5 LMH, respectively. We could not extract a theoretical value for PES and NY membrane flux as their untreated versions are hydrophilic. However, we may comment why the PES flux is not higher compared to PVDF despite its higher porosity, smaller tortuosity and higher pore diameter. We hypothesize that the thicker fluorocarbon film deposition (~100 nm

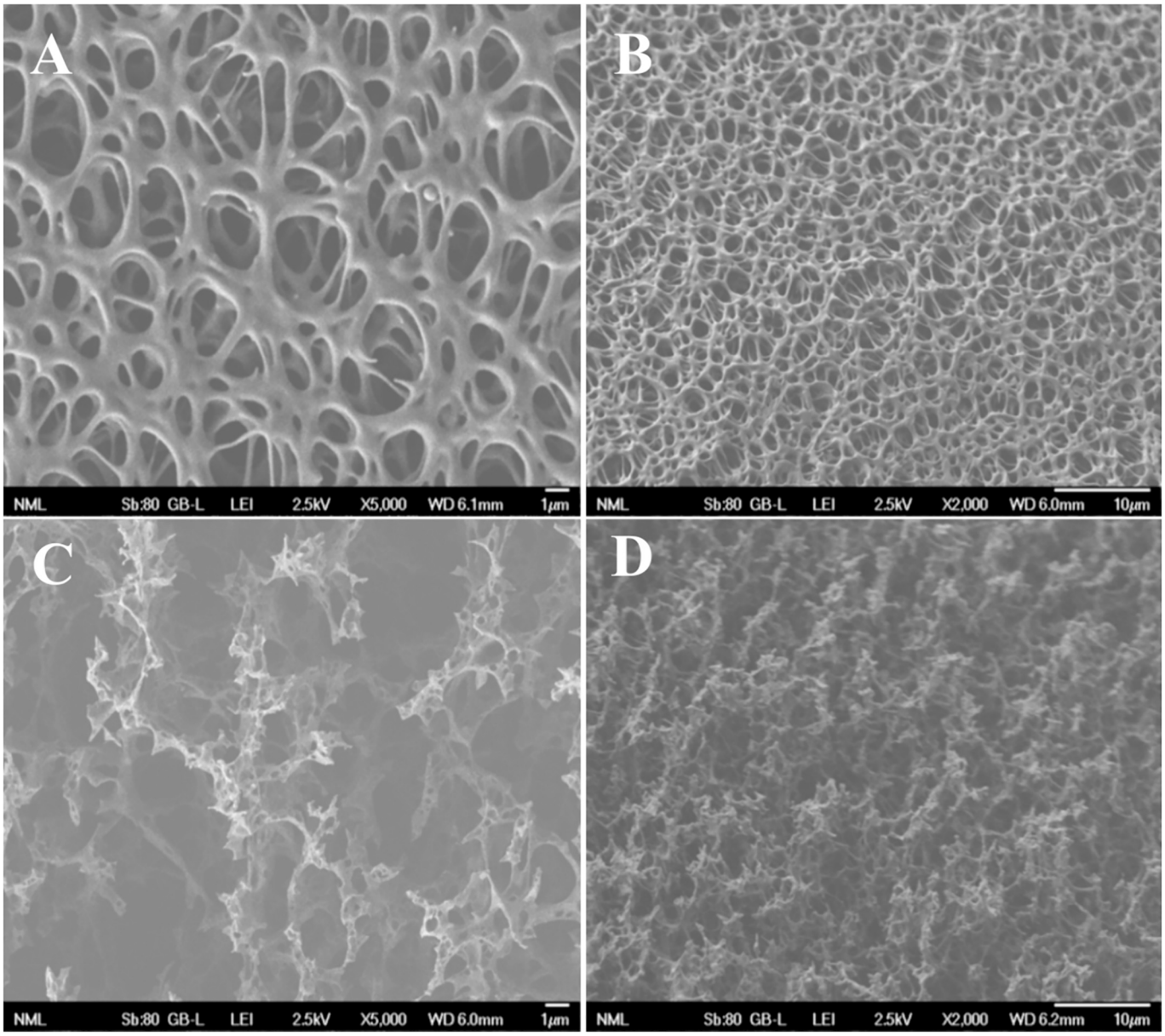

Fig. 3. SEM images of the PES membrane morphology A) Untreated top down (x5000 magnification), B) Untreated at 45° angle (x2000 magnification), C) After treatment for 2:00 min with O_2 top down (x5000 magnification) and D) After treatment for 2:00 min with O_2 at 45° angle (x2000 magnification).

versus ~50 nm for PVDF) narrows significantly the surface pores (as done also in classical PECVD in trenches) thus reducing the vapor flux. For Nylon this phenomenon is also enhanced by the higher values of tortuosity.

Combining these MD results of PES and NY with the MD results from hydrophilic CA (Cellulose Acetate membranes) from our previous work [1] allows us to claim that our technology may provide a replacement of all fluorinated membranes in the near future, contributing to PFAS free / Teflon-free membranes for membrane technologies. One may of course claim that our membranes are not totally PFAS free as we are depositing a fluorocarbon film to change the surface energy. However, the film is very thin (on the order of 100 nm) while the membranes are typically much (1000×) thicker (at least 100 μm). Nevertheless, we are working with other plasma chemistry to substitute even the thin fluorocarbon film for the hydrophobization process, and we plan to demonstrate the results in a future publication to showcase completely PFAS free membrane membranes and membrane processing.

4. Conclusions

In the context of this work, three commercial membranes, PVDF (initially hydrophobic), PES and NY (both initially hydrophilic) were processed using completely dry, plasma technology (plasma nanotexturing followed by plasma hydrophobization). The surface treatment of the membranes aimed at their superhydrophobicity to optimize their properties during a desalination process with a DCMD setup. The three membranes, regardless of their initial wetting properties, were successfully rendered not only superhydrophobic, but also superoleophobic with contact angles >150° and low hysteresis angles <10° for liquids having a surface tension down to 40mN/m, while they remained oleophobic down to 30mN/m. This property may allow their use with low surface tension waste streams and not only saline water.

After fully evaluating the membranes regarding their superhydrophobic properties and morphology, a membrane desalination experiment followed using a DCMD setup. This test showed that in the case of the initially hydrophobic PVDF membrane there was a 13%

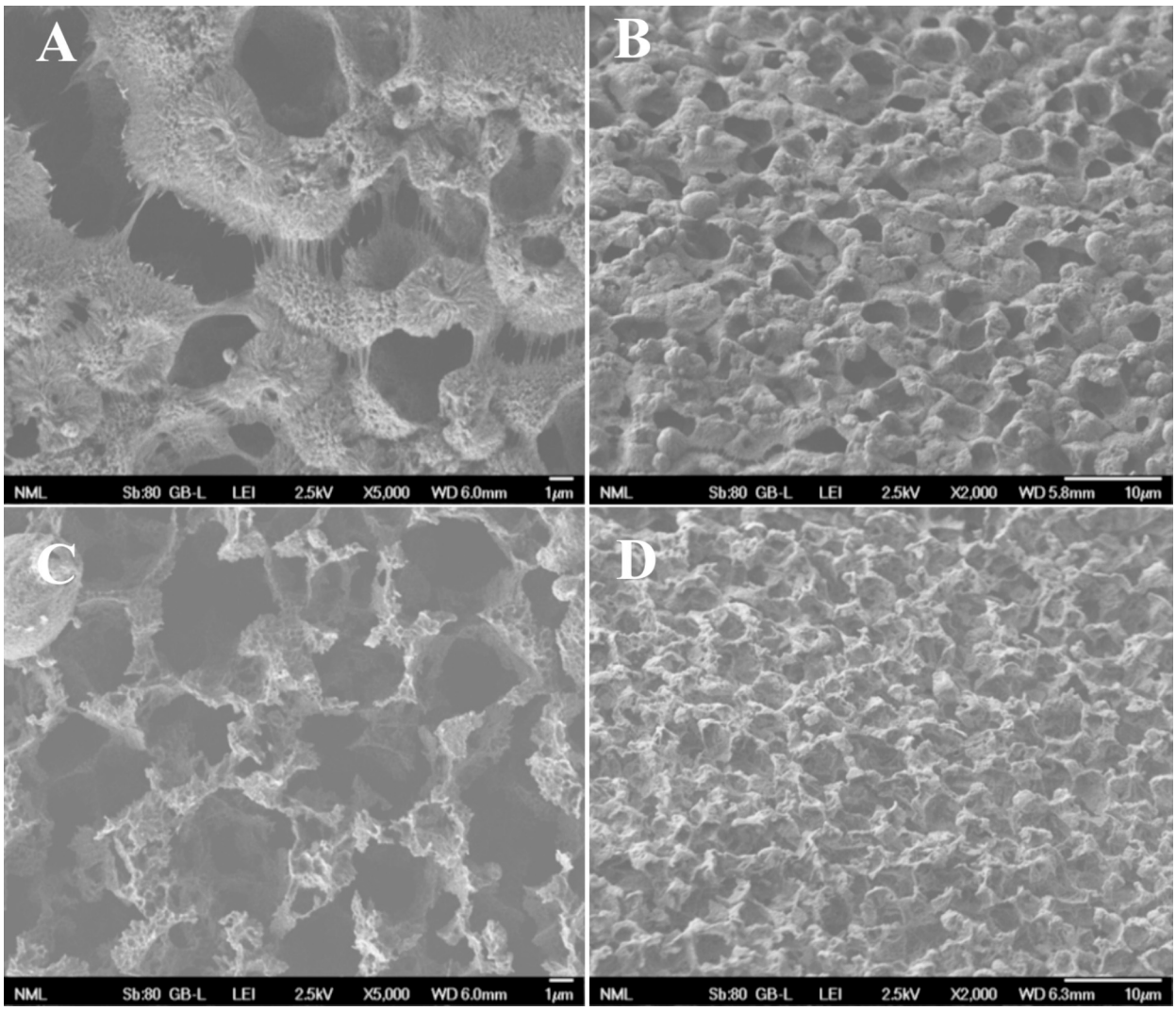

Fig. 4. SEM images of the NY membrane morphology A) Untreated top down (x5000 magnification), B) Untreated at 45° angle (x2000 magnification), C) After treatment for 1:00 min with O_2 top down (x5000 magnification) and D) After treatment for 1:00 min with O_2 at 45° angle (x2000 magnification).

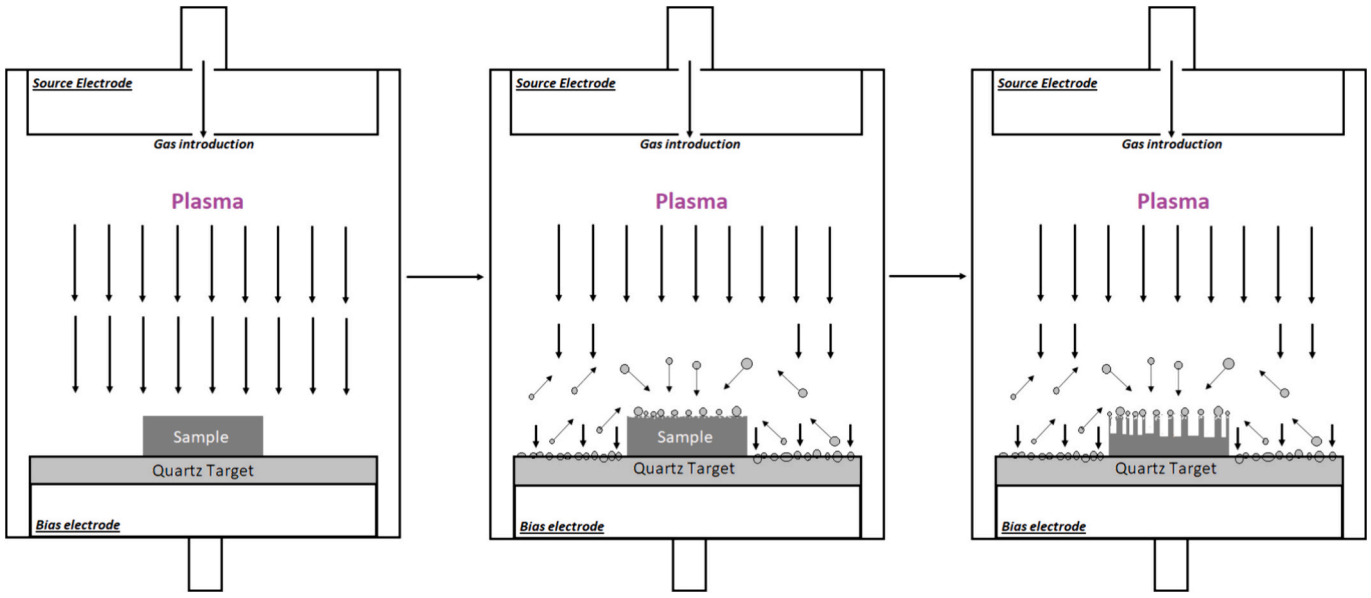

Fig. 5. Schematic illustration of plasma nanotexturing process with O_2 using a quartz target plate.

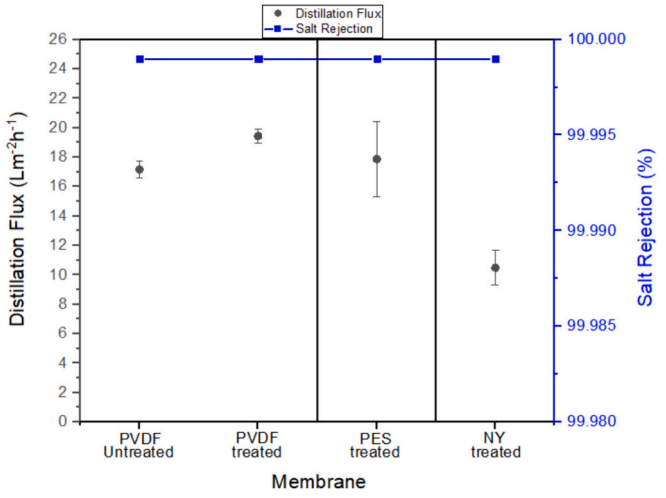

Fig. 6. DCMD experiment results showing the flux increase of the treated PVDF membranes and the successful use for desalination of the initially superhydrophilic PES and NY membranes.

Table 4
Porosity and tortuosity alterations caused by plasma treatment.

Membrane - Pore size	Porosity ε (%)	Tortuosity τ
Untreated PVDF 0.45 μm	66.5 ± 0.8	1.50 ± 0.07
Treated PVDF 0.45 μm 3 min O_2 + 1:30 min C_4F_8	66.6 ± 0.3	1.50 ± 0.06
Untreated PES 1.20 μm	83.9 ± 0.2	1.19 ± 0.04
Treated PES 1.20 μm 2 min O_2 + 3:00 min C_4F_8	86.3 ± 0.2	1.16 ± 0.04
Untreated NY 1.20 μm	58.0 ± 1.5	3.47 ± 0.11
Treated NY 1.20 μm 1 min O_2 + 3:00 min C_4F_8	62.9 ± 1.0	2.99 ± 0.10

increase in permeability flow from 17.2 LMH to 19.4 LMH. At the same time, the originally superhydrophilic PES and NY membranes, which due to their hydrophilic nature were unusable in desalination experiments before treatment, provided a stable desalination performance for at least 2 h and permeability flows of 17.9 LMH for PES and 10.5 LMH for NY. We thus demonstrated PFAS free membranes for MD by transitioning from fluorinated membranes such as PTFE and PVDF to membranes like PES and NY.

Area of interest

Superhydrophobic surfaces, Oleophobic surfaces, Plasma technology, Polymeric membranes, Direct contact membrane distillation (DCMD).

Declaration of competing interest

The authors declare that they have no known competing financial interests or personal relationships that could have appeared to influence the work reported in this paper.

Data availability

Data will be made available on request.

Acknowledgments

Financial support has been provided by the Horizon 2020 EIC Transition project SuperClean no 101099381.

Appendix A. Supplementary data

Supplementary data to this article can be found online at https://doi.org/10.1016/j.mne.2024.100269.

References

[1] D. Ioannou, Y. Hou, P. Shah, K. Ellinas, M. Kappl, A. Sapalidis, V. Constantoudis, H. J. Butt, E. Gogolides, Plasma-induced superhydrophobicity as a green technology for enhanced air gap membrane distillation, ACS Appl. Mater. Interfaces 15 (14) (Apr. 2023) 18493–18504, https://doi.org/10.1021/acsami.3c00535.
[2] S. Porada, R. Zhao, A. Van Der Wal, V. Presser, P.M. Biesheuvel, Review on the science and technology of water desalination by capacitive deionization, Prog. Mater. Sci. 58 (8) (2013) 1388–1442, https://doi.org/10.1016/j.pmatsci.2013.03.005. Elsevier Ltd.
[3] M.M. Mekonnen, A.Y. Hoekstra, Sustainability: four billion people facing severe water scarcity, Sci. Adv. 2 (2) (Feb. 2016), https://doi.org/10.1126/sciadv.1500323.
[4] A.D. Khawaji, I.K. Kutubkhanah, J.M. Wie, Advances in seawater desalination technologies, Desalination 221 (1–3) (Mar. 2008) 47–69, https://doi.org/10.1016/j.desal.2007.01.067.
[5] D. Nioras, K. Ellinas, V. Constantoudis, E. Gogolides, How different are fog collection and dew water harvesting on surfaces with different wetting behaviors? ACS Appl. Mater. Interfaces 13 (40) (Oct. 2021) 48322–48332, https://doi.org/10.1021/acsami.1c16609.
[6] D. Nioras, K. Ellinas, E. Gogolides, Atmospheric water harvesting on micro-nanotextured biphilic surfaces, ACS Appl. Nano Mater. 5 (8) (Aug. 2022) 11334–11341, https://doi.org/10.1021/acsanm.2c02439.
[7] K.W. Lawson, D.R. Lloyd, PII: S0376-7388(96)00236–0, 1997.
[8] M. Rezaei, D.M. Warsinger, J.H. Lienhard V, M.C. Duke, T. Matsuura, W. M. Samhaber, Wetting phenomena in membrane distillation: mechanisms, reversal, and prevention, Water Res. 139 (Aug. 01, 2018) 329–352, https://doi.org/10.1016/j.watres.2018.03.058. Elsevier Ltd.
[9] A. Alkhudhiri, N. Darwish, N. Hilal, Membrane distillation: a comprehensive review, Desalination 287 (Nov. 15, 2012) 2–18, https://doi.org/10.1016/j.desal.2011.08.027.
[10] A. Sadeghzadeh, S. Bazgir, M.M.A. Shirazi, Fabrication and characterization of a novel hydrophobic polystyrene membrane using electroblowing technique for desalination by direct contact membrane distillation, Sep. Purif. Technol. 239 (May 2020), https://doi.org/10.1016/j.seppur.2019.116498.
[11] L.D. Tijing, Y.C. Woo, W.G. Shim, T. He, J.S. Choi, S.H. Kim, H.K. Shon, Superhydrophobic nanofiber membrane containing carbon nanotubes for high-performance direct contact membrane distillation, J. Membr. Sci. 502 (Mar. 2016) 158–170, https://doi.org/10.1016/j.memsci.2015.12.014.
[12] B.A. Cinelli, D.M.G. Freire, F.A. Kronemberger, Membrane distillation and pervaporation for ethanol removal: are we comparing in the right way? Sep. Sci. Technol. (Philadelphia) 54 (1) (Jan. 2019) 110–127, https://doi.org/10.1080/01496395.2018.1498518.
[13] T. Horseman, Y. Yin, K.S. Christie, Z. Wang, T. Tong, S. Lin, Wetting, scaling, and fouling in membrane distillation: state-of-the-art insights on fundamental mechanisms and mitigation strategies, ACS ES&T Eng. 1 (1) (Jan. 2021) 117–140, https://doi.org/10.1021/acsestengg.0c00025.
[14] J. Jung, Y. Shin, Y.J. Choi, J. Sohn, S. Lee, K. An, Hydrophobic surface modification of membrane distillation (MD) membranes using water-repelling polymer based on urethane rubber, Desal. Water Treat 57 (22) (May 2016) 10031–10041, https://doi.org/10.1080/19443994.2015.1038111.
[15] H. Chamani, J. Woloszyn, T. Matsuura, D. Rana, C.Q. Lan, Pore wetting in membrane distillation: a comprehensive review, Prog. Mater. Sci. 122 (Oct. 01, 2021), https://doi.org/10.1016/j.pmatsci.2021.100843. Elsevier Ltd.
[16] F. He, J. Gilron, H. Lee, L. Song, K.K. Sirkar, Potential for scaling by sparingly soluble salts in crossflow DCMD, J. Membr. Sci. 311 (1–2) (Mar. 2008) 68–80, https://doi.org/10.1016/j.memsci.2007.11.056.
[17] M. Gryta, Studies of membrane scaling during water desalination by membrane distillation, Chem. Pap. 73 (3) (Mar. 2019) 591–600, https://doi.org/10.1007/s11696-018-0628-y.
[18] Ioannou Dimosthenis, Shah Prexa, Ellinas Kosmas, Kappl Michael, Sapalidis Andreas, Butt Hans Jurgen, Gogolides Evangelos, Antifouling plasma-treated membranes with stable superhydrophobic properties for membrane distillation, ACS Appl. Polym. Mater. 5 (12) (2023) 9785–9795.
[19] A.A. Puranik, L.N. Rodrigues, J. Chau, L. Li, K.K. Sirkar, Porous hydrophobic-hydrophilic composite membranes for direct contact membrane distillation, J. Membr. Sci. 591 (Dec. 2019), https://doi.org/10.1016/j.memsci.2019.117225.
[20] A.K. Sharma, A. Juelfs, C. Colling, S. Sharma, S.P. Conover, A.A. Puranik, J. Chau, L. Rodrigues, K.K. Sirkar, Porous hydrophobic–hydrophilic composite hollow fiber and flat membranes prepared by plasma polymerization for direct contact membrane distillation, Membranes (Basel) 11 (2) (Feb. 2021) 1–16, https://doi.org/10.3390/membranes11020120.
[21] L. Li, L. Song, K.K. Sirkar, Desalination performances of large hollow fiber-based DCMD devices, Ind. Eng. Chem. Res. 56 (6) (Feb. 2017) 1594–1603, https://doi.org/10.1021/acs.iecr.6b04037.
[22] L. Song, Z. Ma, X. Liao, P.B. Kosaraju, J.R. Irish, K.K. Sirkar, Pilot plant studies of novel membranes and devices for direct contact membrane distillation-based desalination, J. Membr. Sci. 323 (2) (Oct. 2008) 257–270, https://doi.org/10.1016/j.memsci.2008.05.079.

[23] D. Singh, L. Li, G. Obusckovic, J. Chau, K.K. Sirkar, Novel cylindrical cross-flow hollow fiber membrane module for direct contact membrane distillation-based desalination, J. Membr. Sci. 545 (2018) 312–322, https://doi.org/10.1016/j.memsci.2017.09.007.
[24] D. Ioannou, P. Shah, K. Ellinas, M. Kappl, A. Sapalidis, H.J. Butt, E. Gogolides, Antifouling plasma-treated membranes with stable superhydrophobic properties for membrane distillation, ACS Appl. Polym. Mater. 5 (12) (Dec. 2023) 9785–9795, https://doi.org/10.1021/acsapm.3c01512.
[25] Y. Hou, P. Shah, V. Constantoudis, E. Gogolides, M. Kappl, H.J. Butt, A super liquid-repellent hierarchical porous membrane for enhanced membrane distillation, Nat. Commun. 14 (1) (Dec. 2023), https://doi.org/10.1038/s41467-023-42204-7.
[26] Dorsan Filtration, Dorsan Living Filtration , Microfiltration Memrabranes. https://www.dorsanfiltration.com/en/product/microfiltration-membranes/, 2024.
[27] A. Zeniou, A. Smyrnakis, V. Constantoudis, K. Awsiuk, E. Gogolides, One-step control of hierarchy and functionality of polymeric surfaces in a new plasma nanotechnology reactor, Nanotechnology 32 (23) (Jun. 2021), https://doi.org/10.1088/1361-6528/abe6ca.
[28] E. Balis, A. Sapalidis, G. Pilatos, E. Kouvelos, C. Athanasekou, C. Veziri, P. Boutikos, K.G. Beltsios, G. Romanos, Enhancement of vapor flux and salt rejection efficiency induced by low cost-high purity MWCNTs in upscaled PVDF and PVDF-HFP hollow fiber modules for membrane distillation, Sep. Purif. Technol. 224 (March) (2019) 163–179, https://doi.org/10.1016/j.seppur.2019.04.067.
[29] M.C. García-Payo, M.A. Izquierdo-Gil, C. Fernández-Pineda, Wetting study of hydrophobic membranes via liquid entry pressure measurements with aqueous alcohol solutions, J. Colloid Interface Sci. 230 (2) (2000) 420–431, https://doi.org/10.1006/jcis.2000.7106.
[30] A. Lee, J.W. Elam, S.B. Darling, Membrane materials for water purification: design, development, and application, Environ. Sci. (Camb) 2 (1) (2016) 17–42, https://doi.org/10.1039/c5ew00159e.
[31] J.S. Mackie, P. Meares, The diffusion of electrolytes in a cation-exchange resin membrane I. Theoretical, Proc. R. Soc. Lond. A Math. Phys. Sci. 232 (1191) (1955) 498–509, https://doi.org/10.1098/rspa.1955.0234.
[32] S.B. Iversen, V.K. Bhatia, K. Dam-Johansen, G. Jonsson B', Characterization of microporous membranes for use in membrane contactors, 1997.
[33] D.U. Lawal, A.E. Khalifa, Flux prediction in direct contact membrane distillation, Int. J. Mater. Mech. Manuf. 2 (4) (2014) 302–308, https://doi.org/10.7763/ijmmm.2014.v2.147.
[34] L. Li, K.K. Sirkar, Influence of microporous membrane properties on the desalination performance in direct contact membrane distillation, J. Membr. Sci. 513 (Sep. 2016) 280–293, https://doi.org/10.1016/j.memsci.2016.04.015.
[35] D. Ioannou, A. Sapalidis, E. Gogolides, White light reflectance spectroscopy as a novel and noninvasive method for in situ wetting monitoring in membrane distillation, Desalination 574 (2024).
[36] J. Qi, J. Lv, W. Bian, J. Li, S. Liu, Experimental study on the membrane distillation of highly mineralized mine water, Int. J. Coal Sci. Technol. 8 (5) (2021) 1025–1033, https://doi.org/10.1007/s40789-021-00432-6.
[37] K. Ellinas, A. Tserepi, E. Gogolides, From superamphiphobic to amphiphilic polymeric surfaces with ordered hierarchical roughness fabricated with colloidal lithography and plasma nanotexturing, Langmuir 27 (7) (Apr. 2011) 3960–3969, https://doi.org/10.1021/la104481p.
[38] K. Ellinas, A. Tserepi, E. Gogolides, Superhydrophobic fabrics with mechanical durability prepared by a two-step plasma processing method, Coatings 8 (10) (2018), https://doi.org/10.3390/COATINGS8100351.
[39] A. Zeniou, A. Smyrnakis, V. Constantoudis, K. Awsiuk, E. Gogolides, One-step control of hierarchy and functionality of polymeric surfaces in a new plasma nanotechnology reactor, Nanotechnology 32 (23) (2021).
[40] A.K. Gnanappa, D.P. Papageorgiou, E. Gogolides, A. Tserepi, A.G. Papathanasiou, A.G. Boudouvis, Hierarchical, plasma nanotextured, robust superamphiphobic polymeric surfaces structurally stabilized through a wetting-drying cycle, Plasma Process. Polym. 9 (3) (Mar. 2012) 304–315, https://doi.org/10.1002/ppap.201100124.
[41] K. Tsougeni, N. Vourdas, A. Tserepi, E. Gogolides, C. Cardinaud, Mechanisms of oxygen plasma nanotexturing of organic polymer surfaces: from stable super hydrophilic to super hydrophobic surfaces, Langmuir 25 (19) (Oct. 2009) 11748–11759, https://doi.org/10.1021/la901072z.
[42] K. Ellinas, A. Tserepi, E. Gogolides, Durable superhydrophobic and superamphiphobic polymeric surfaces and their applications: a review, Adv. Colloid Interf. Sci. 250 (Dec. 01, 2017) 132–157, https://doi.org/10.1016/j.cis.2017.09.003. Elsevier B.V.
[43] M. K, T. Matsuura, Membrane distillation principles and applications, 2011.
[44] R.W. Schofield, A.G. Fane, C.J.D. Fell, R. Macoun, Factors affecting flux in membrane distillation, Desalination 77 (C) (1990) 279–294, https://doi.org/10.1016/0011-9164(90)85030-E.
[45] R.W. Field, H.Y. Wu, J.J. Wu, Multiscale modeling of membrane distillation: some theoretical considerations, Ind. Eng. Chem. Res. 52 (26) (2013) 8822–8828, https://doi.org/10.1021/ie302363e.
[46] M. Khayet, A. Velázquez, J.I. Mengual, Modelling mass transport through a porous partition: effect of pore size distribution, J. Non-Equilib. Thermodyn. 29 (3) (2004) 279–299, https://doi.org/10.1515/JNETDY.2004.055.